Desalination and Water Treatment
www.deswater.com
doi: 10.5004/dwt.2021.27096

222 (2021) 416–425
May

Effect of coexistent anions on the nitrate removal by denitrifying granular sludge

Yankai Guo[a], Chao Zhang[a,c], Weilong Liu[a], Yaoqi Xue[a,d], Jing Lian[a,*], Jianbo Guo[b,*], Yanyan Niu[a]

[a]*School of Environmental Science and Engineering & Pollution Prevention Biotechnology Laboratory of Hebei Province, Hebei University of Science and Technology, Yuhua East Road 70#, Shijiazhuang 050018, China, Tel. +86 18931170850; emails: ningjingzhiyuan98@163.com (J. Lian), kedagyk@sina.com (Y. Guo), 15690327278@163.com (C. Zhang), Natureliu539@163.com (W. Liu), doudounbamvp@163.com (Y. Xue), niu1577118337@163.com (Y. Niu)*
[b]*Tianjin Key Laboratory of Aquatic Science and Technology, School of Environmental and Municipal Engineering, Tianjin Chengjian University, Jinjing Road 26#, Tianjin 300384, China, Tel. +86 22 23085116; email: jianbguo@163.com*
[c]*School of Environment Science and Engineering, Tianjin University, Tianjin 300350, China*
[d]*CSD Water Service Co., Ltd., Hebei branch, Yuhua East Road 133#, Shijiazhuang 050000, China*

Received 3 February 2020; Accepted 31 January 2021

A B S T R A C T

Coexistent anions are the main limiting factors in nitrate (NO_3^-) removal process in both ground and surface waters. The effect of nitrite (NO_2^-) and perchlorate (ClO_4^-) on NO_3^- removal via denitrifying granular sludge was investigated herein. The results indicate that the nitrate removal rate (NRR) decreased from 2.73 to 1.94 kg N m^{-3} d^{-1} with an increasing NO_2^- concentration from 150 to 300 mg L^{-1}. However, the NRR reached 2.09 kg N m^{-3} d^{-1} at a NO_2^- concentration of 450 mg L^{-1}. Moreover, the NRR gradually decreased from 2.77 to 1.87 kg N m^{-3} d^{-1} with increasing ClO_4^- concentration (100–900 mg L^{-1}). In the presence of coexisting anions, the decrease in biomass, disintegration of granules, and increase in shear sensitivity (K_{SS}) deteriorated the characteristics of granules, resulting in a decrease in the NRR. Further, a correlation analysis indicated that NRR and shear sensitivity are significantly negatively correlated.

Keywords: Nitrate removal; Denitrifying granular sludge; Coexistent anions; Correlation analysis

1. Introduction

A continuous increase in the concentration of nitrate (NO_3^-) has been observed in ground and surface waters (rivers and lakes) as a result of intensified agriculture, industrialization, and urbanization. The World Health Organization stipulates that the maximum nitrate–nitrogen (NO_3^-–N) concentration in drinking water is 10 mg N L^{-1}, in which any higher concentration is harmful to human health because of its contribution to methemoglobinemia, gastric cancer, and non-Hodgkin lymphoma [1]. Among the current remediation technologies, biological denitrification is one of the most economical and widely used. Denitrifying bacteria (DB) that are universally present in the environment can use NO_3^- as a terminal electron acceptor under anoxic conditions [2]. Over the past 30 y, several novel denitrification technologies have been proposed [3,4]. The feasibility and efficiency of these biological technologies in removing highly loaded nitrogenous effluents have been studied [5,6]. Denitrifying granular sludge (DGS) is an important method as achieves high efficiency,

* Corresponding author.

energy conservation, and equipment miniaturization for biological wastewater treatment [3].

With the exception of NO_3^-, anions, such as nitrite (NO_2^-) and perchlorate (ClO_4^-), been detected in the groundwater and soil near manufactures of solid rocket fuel, propellants, fireworks, munitions, matches, signal flares, and other commercial products [7,8]. These anions have different effects on the nitrate removal rate (NRR) and the structure or metabolic activities of the DGS. In particular, NO_2^- that is accumulated during denitrification is harmful to the DGS [9]. Previous research found that nitrite–nitrogen (NO_2^-–N) might cause the formation of free nitrous acid, which may inhibit denitrification [10]. In addition, various studies have shown that the reduction of ClO_4^- is inhibited in the presence of NO_3^- [11,12]. Van Ginkel et al. [13] found that many perchlorate-reducing enzymes of perchlorate-reducing bacteria were suppressed by NO_3^-. However, the removal of NO_3^- by DGS in the presence of ClO_4^- has not been systematically studied. During the biodegradation of ClO_4^-, oxygen is produced, which destroys, to a certain extent, the anoxic or anaerobic environment in the sludge, thereby inhibiting the microorganism activity [14]. Thus, the presence of ClO_4^- affects the removal of NO_3^- by DGS. To date, most studies have focused on the simultaneous removal of coexisting anions in bioreactors [1,11].

Granule characteristics are significant factors in reactor performance. Tang et al. [15] found that a high biomass concentration is a key factor for pollutant removal. Sheng et al. [16] showed that the shear sensitivity (K_{SS}) of granules has a crucial influence on the long-term stable operation of sludge reactors. Verawaty et al. [17] indicated that granules must have optimal granular sludge sizes and that much larger or smaller sizes are not conducive to the settlement ability and reactor performance. Further, extracellular polymeric substances (EPS) play an important role in the surface characteristics of granules [3], protecting the granules in difficult environments. However, few studies have investigated the characteristics of DGS under coexisting anion (NO_2^- and ClO_4^-) conditions.

Accordingly, the objectives of this study are: (1) to study the effect of coexistent anions (NO_2^- and ClO_4^-) on the performance of NO_3^- removal; (2) to explore the effects of coexisting anions (NO_2^- and ClO_4^-) on the physicochemical (biomass, sludge volume index (SVI), mass percentage, and K_{SS}) and surface characteristics (EPS, protein (PN), polysaccharide (PS), and PN/PS) of the DGS; and (3) to investigate the correlation between the operational and environmental conditions and sludge characteristics. The results of this study will provide useful information for the application of DGS in the treatment of NO_3^- wastewater.

2. Materials and methods

2.1. Reactor, wastewater, and seed sludge

Four identical Plexiglas up-flow anaerobic sludge blanket (UASB) column reactors (R_N, R_{NN}, R_{NP}, and R_{NNP}) 60 cm high with internal diameters of 6.8 cm and equipped with three-phases were fabricated and set up (Fig. S1) in order to determine the effects of coexisting NO_2^- and ClO_4^- on NRR. Synthetic NO_3^-, NO_2^-, and ClO_4^- contaminated waters were prepared using sodium nitrate, sodium nitrite, and sodium perchlorate as contaminants. A microelement solution (1.0 mL L^{-1}) was added to the influent, which contained 63.7 mL L^{-1} of $C_{10}H_{14}N_2Na_2O_8{\cdot}2H_2O$, 5.5 mL L^{-1} of $ZnSO_4$, 5.0 mL L^{-1} of $FeSO_4{\cdot}7H_2O$, 4.3 mL L^{-1} of $MnSO_4$, 2.2 mL L^{-1} of $ZnSO_4$, 1.6 mL L^{-1} of $CoC_{12}{\cdot}6H_2O$, 1.6 mL L^{-1} of $CuSO_4{\cdot}5H_2O$, and 1.6 mL L^{-1} of $Na_2MoO_4{\cdot}2H_2O$. The DGS was obtained from a laboratory-scale UASB reactor that was fed with sodium nitrate as the electron acceptor and methanol as the electron donor [3]. The mixed liquor suspended solids (MLSS), mixed liquor volatile suspended solids (MLVSS), K_{SS}, SVI, and the main mass percentage of granules were 49.37 ± 2.47 g L^{-1}, 15.84 ± 0.80 g L^{-1}, 0.001748 ± 0.0001, 15.76 ± 0.79 mL g^{-1}, and 1–2 mm, respectively. The experimental temperature was set to 30°C ± 2°C.

2.2. UASB bioreactor operation

The experiment was conducted for 30 d, in which the four reactors were operated in parallel. The main input variables were the species and concentrations of coexisting anions, including NO_2^-, ClO_4^-, and NO_2^- and ClO_4^-. The operational characteristics of the four reactors are listed in Table 1.

2.3. Shear sensitivity analysis

The shear sensitivity of the sludge was characterized using the K_{SS} parameter, which is defined as:

$$K_{ss} = \frac{m_{d,\infty}}{m_T} \quad (1)$$

where $m_{d,\infty}$ is the dispersed particle concentration of the small particles, as defined by Mikkelsen and Keiding [18], and was measured when the shear experiments reached equilibrium, in which the total MLVSS of the granular sludge sample (m_T) was 5 g L^{-1} at G = 800 s^{-1}. A baffled paddle-mixing cylindrical reactor with dimensions of 58.2 mm × 83.2 mm (inner diameter × height) was used to perform a shear test, wherein the reactor was placed in a stink cupboard at a room temperature of 30°C ± 2°C.

2.4. Other analysis methods

Concentrations of ClO_4^-, NO_3^-, and NO_2^- were quantified using an ion chromatograph (DX120; Dionex, Sunnyvale, CA, USA) equipped with a Dionex IonPac AS20 analytical column (4 mm × 250 mm) and an AG20 guard column (4 mm × 50 mm), a self-regenerating suppressor, and an autosampler. ClO_4^-, NO_3^-, and NO_2^- were measured using a 40 mmol L^{-1} KOH eluent.

The MLSS, MLVSS, SVI, and mass percentage granules measurements were taken using the American Public Health Association (APHA) standard methods [19]. The EPS from the activated sludge and granules were extracted using the heat extraction method [20]. The PN and PS concentrations were determined using the Bradford method [21] and the anthrone-sulfuric acid method [3], respectively.

Table 1
Operational condition of the reactors

Reactors	Phase I			Phase II			Phase III		
	NO_3^-–N (mg L^{-1})	NO_2^-–N (mg L^{-1})	ClO_4^- (mg L^{-1})	NO_3^-–N (mg L^{-1})	NO_2^-–N (mg L^{-1})	ClO_4^- (mg L^{-1})	NO_3^-–N (mg L^{-1})	NO_2^-–N (mg L^{-1})	ClO_4^- (mg L^{-1})
R_N	500			500			500		
R_{NN}	500	150		500	300		500	450	
R_{NP}	500		100	500		300	500		900
R_{NNP}	500	150	100	500	300	300	500	450	900

Reactor (R_N) without additional coexistent anions served as control;
Reactors added with NO_2^-, ClO_4^-, and NO_2^- and ClO_4^- were designated as R_{NN}, R_{NP}, and R_{NNP}.

2.5. Data analysis

The graph and data processing was completed using OriginPro 8.0, and Microsoft Excel, respectively. A least significant difference multiple range tests was used to determine the statistical significance ($P < 0.05$) between pairs using statistical product and service solutions (SPSS).

3. Results and discussion

3.1. Reactor performance

3.1.1. Nitrate removal rate

The NRR was used to describe the effect of NO_2^- and ClO_4^- on NO_3^- removal during operation. The changes in the NRRs of the four reactors during operation are shown in Fig. 1. The average NRRs of R_N during the three phases were 2.81, 2.56, and 2.25 kg N m^{-3} d^{-1}, respectively. The observed decrease in NRR is related to the increase in biomass in the granular sludge.

To understand the effect of NO_2^- on the DGS, the NRRs of the R_{NN} were explored (Fig. 1b). The average NRRs of R_{NN} during the three phases were 2.73, 1.94, and 2.09 kg N m^{-3} d^{-1}, respectively. These results indicate that the average NRRs decreased when the concentration of NO_2^- changed from 150 to 300 mg L^{-1} (phases I and II, respectively). Conversely, when the NO_2^- concentration reached 450 mg L^{-1} in phase III, the average NRRs increased. The complete degradation of NO_3^- requires nitrate reductase (NaR), nitrite reductase (NiR), nitric oxide reductase,

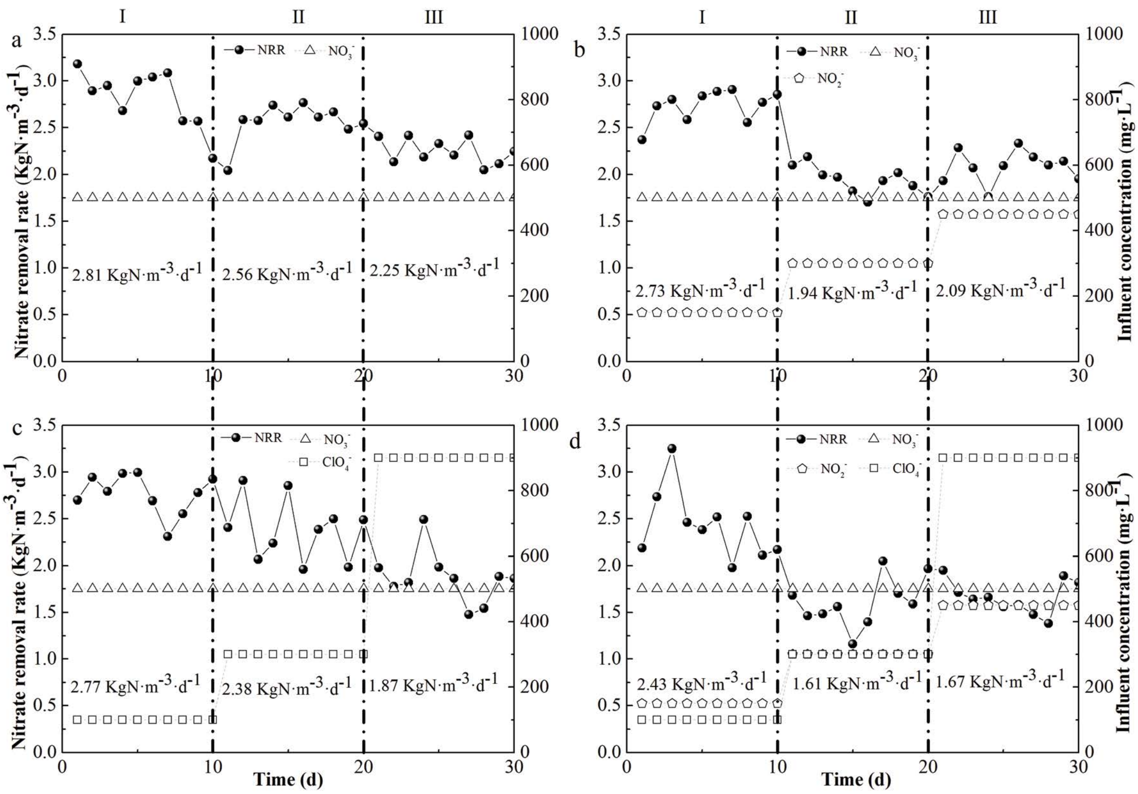

Fig. 1. Change in the NRR during operation: (a) R_N, (b) R_{NN}, (c) R_{NP}, and (d) R_{NNP}.

and nitrous oxide reductase to exist in the DB [22]. Previous studies have shown that different NO_2^- concentrations have different effects on reductase [23]. During the denitrification process, the synthesis of NaR and NiR is induced by high concentrations of NO_2^- (500 mg L^{-1}) [24,25]. However, some other studies have shown that low NO_2^- concentrations limit the expression of NaR, NiR, and nitrous oxide reductase at a NO_2^- concentration of 200 mg L^{-1} [10,26]. This is consistent with our research results. Low NO_2^- concentrations inhibit NO_3^- removal, whereas high concentrations promote NO_3^- removal. Thus, the expression of NaR, NiR, and nitrous oxide reductase might be inhibited at 150 and 300 mg L^{-1} NO_2^-. Conversely, the inhibitory effect of NO_2^- was weakened at 450 mg L^{-1} NO_2^-.

To understand the effect of ClO_4^- on DGS, the NRR of R_{NP} was evaluated (Fig. 1c). The average NRRs of R_{NP} during the three phases were 2.77, 2.38, and 1.87 kg N m^{-3} d^{-1}, respectively. The NRR of R_{NP} decreased with increasing ClO_4^- concentration. This is mainly because microorganisms can reduce ClO_4^- to Cl^- and O_2. This O_2 could inhibit the growth of DB that survived in the anoxic environment [27,28]. Thus, ClO_4^- had a distinct inhibitory effect on the NRRs in each phase.

To understand the effects of NO_2^- and ClO_4^- on the DGS, the NRRs of R_{NNP} were examined (Fig. 1d). The average NRRs of R_{NNP} in the three phases were 2.43, 1.61, and 1.67 kg N m^{-3} d^{-1}, respectively. These results indicate that the coexisting NO_2^- and ClO_4^- have adverse effects on NO_3^- removal in phases I and II. Meanwhile, in phase III, their inhibitory effect was weakened as the concentration of NO_2^- increased to 450 mg L^{-1}, which is similar to the results of R_{NN}.

3.1.2. Nitrate removal stability

The relative standard deviations (RSD) of the specific nitrate removal rate for three consecutive days (RSD-N_3) were used to describe the properties of nitrate removal stability during operation. The changes in the RSD-N_3 of the four reactors during operation are illustrated in Fig. 2. Overall, the RSD-N_3 values decreased during the three phases. The DGS in the R_N, R_{NN}, and R_{NNP} adapted to the new operating environments, resulting in NO_3^- stability. Conversely, in the R_{NP}, RSD-N_3 decreased from 7.11% (phase I) to 2.17% (phase II), and then increased to 7.00% (phase III) (Fig. 2c). This result indicates that the NO_3^- removal stability deteriorated in the presence of high-strength ClO_4^-. Further, NO_3^- removal was slightly inhibited by NO_2^-, and significantly inhibited by ClO_4^-. In addition, NO_2^- had little effect on the removal stability of NO_3^-, whereas ClO_4^- had a significant influence on the stability of NO_3^- removal. Thus, the reactor performance was mainly related to granular sludge characteristics. To further explore the NO_3^- removal performance of DGS in NO_2^- and ClO_4^- conditions, the

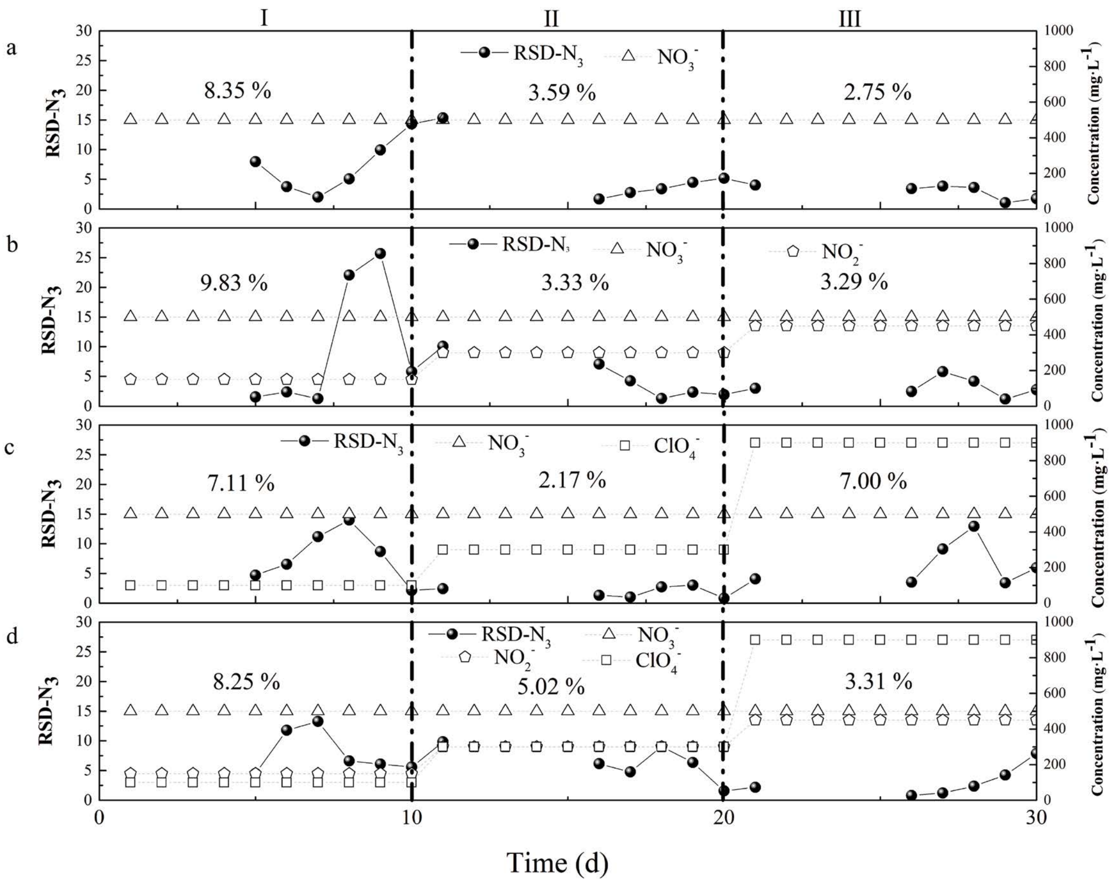

Fig. 2. Change in the RSD-N_3 during operation: (a) R_N, (b) R_{NN}, (c) R_{NP}, and (d) R_{NNP}.

physicochemical and surface characteristics of DGS were investigated.

3.2. Physicochemical characteristics of DGS

3.2.1. Biomass and settling ability of DGS

The MLSS and MLVSS content represented the biomass, determining the concentration of granules in the reactor, while the SVI was representative of settlement performance. The MLSS, MLVSS, and SVI concentrations in each reactor during operation are shown in Fig. 3. The MLVSS accounted for 24.64 ± 1.23 g L^{-1}, 28.81 ± 1.44 g L^{-1}, and 35.48 ± 1.77 g L^{-1} in R_N (Fig. 3a) during the three phases, respectively. Thus, the MLVSS concentration in R_N gradually increased, which may be related to a relatively stable growth environment. In addition, the MLVSS of the other reactors maintained high concentrations in phases I and II before the biomass decreased significantly in phase III. The MLSS trend was similar to that of the MLVSS. The number of cell deaths was related to coexisting anions. Thus, with gradually increasing concentration, there were decreases in biomass [29]. The SVI values of the four reactors maintained stability during operation, indicating that they had good settlement performance.

The specific nitrate removal rate (SNRR) was used to describe the specific activities of the granules and the effects of NO_2^- and ClO_4^- on NO_3^- removal during operation. The SNRRs of the four reactors during operation are shown in Fig. S2. The SNRRs in R_N were 0.0398, 0.0252 and 0.0234 kg N $gVSS^{-1}$ m^{-3} d^{-1} in the three phases, respectively. In R_{NN}, the SNRRs were accounted for 0.0380, 0.0239, and 0.0255 kg N $gVSS^{-1}$ m^{-3} d^{-1}, indicating that NO_2^- would inhibit the bacterial activity. Meanwhile, in R_{NP}, the SNRRs were 0.0359, 0.0230, and 0.0204 kg N $gVSS^{-1}$ m^{-3} d^{-1}, which indicates that ClO_4^- inhibits the activity of bacteria during operation. In R_{NNP}, the SNRRs were 0.0362, 0.0192, and 0.0207 kg N $gVSS^{-1}$ m^{-3} d^{-1}, which are similar those of the R_{NN}. In addition, the SNRR trend was consistent with that of the NRR.

3.2.2. Mass percentage of DGS

The particle size of the granules critically affected the physicochemical characteristics. The mass percentages of the granules in the four reactors during operation are illustrated in Fig. 4. Over the three phases, the mass percentage of granules within R_N increased, within granules in the range of 2.0–4.8 mm increased from 17.89% ± 0.89% (phase I) to 37.50% ± 1.88% (phase II) to 45.72% ± 2.29% (phase III). This result indicates that a large amount of microorganisms grow under favourable conditions, resulting in an increasing granule particle size. The mass percentages of granules in R_{NN}, R_{NP}, and R_{NNP} exhibited a downward

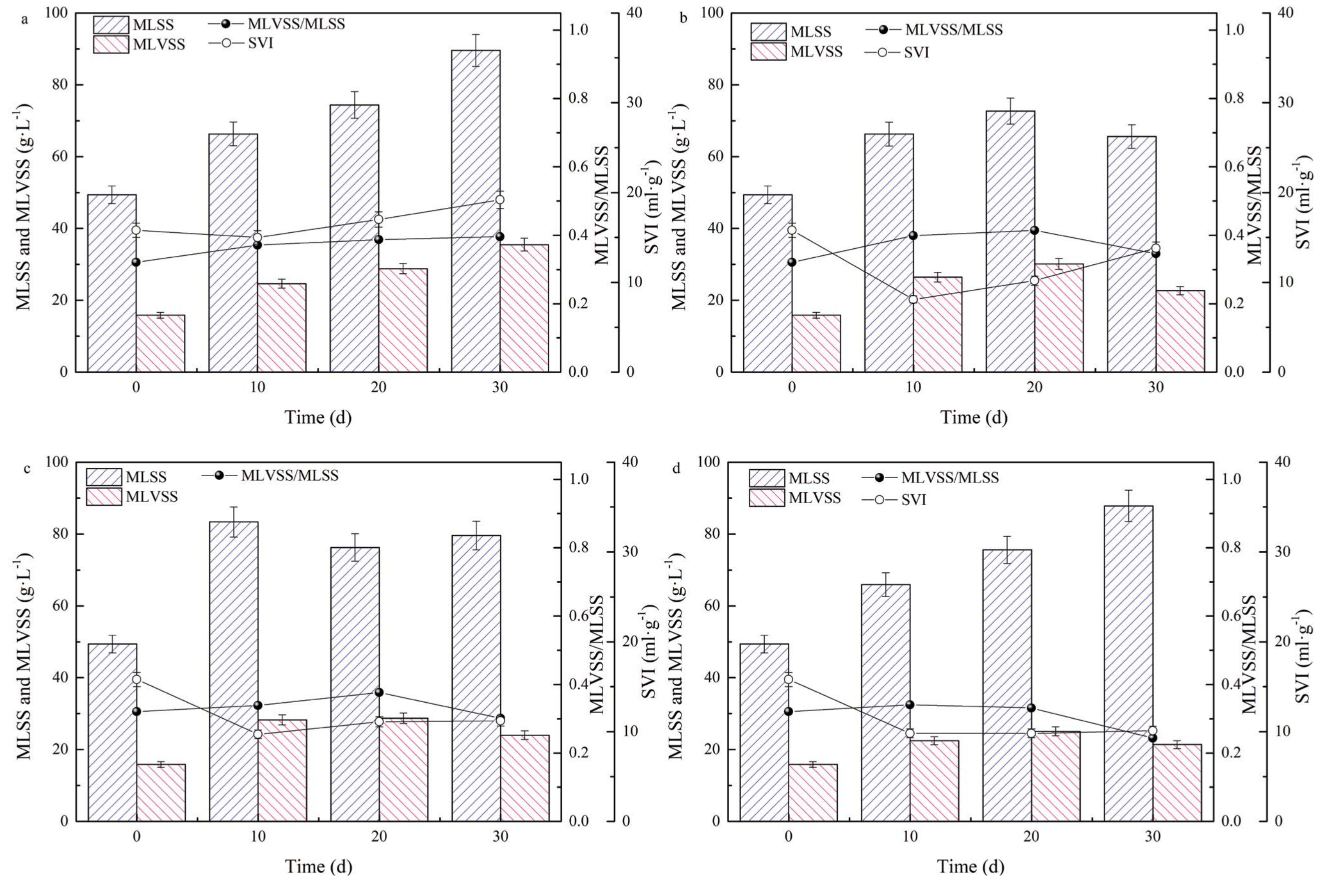

Fig. 3. Change in the MLSS, MLVSS, MLVSS/MLSS and SVI during operation: (a) R_N, (b) R_{NN}, (c) R_{NP}, and (d) R_{NNP}.

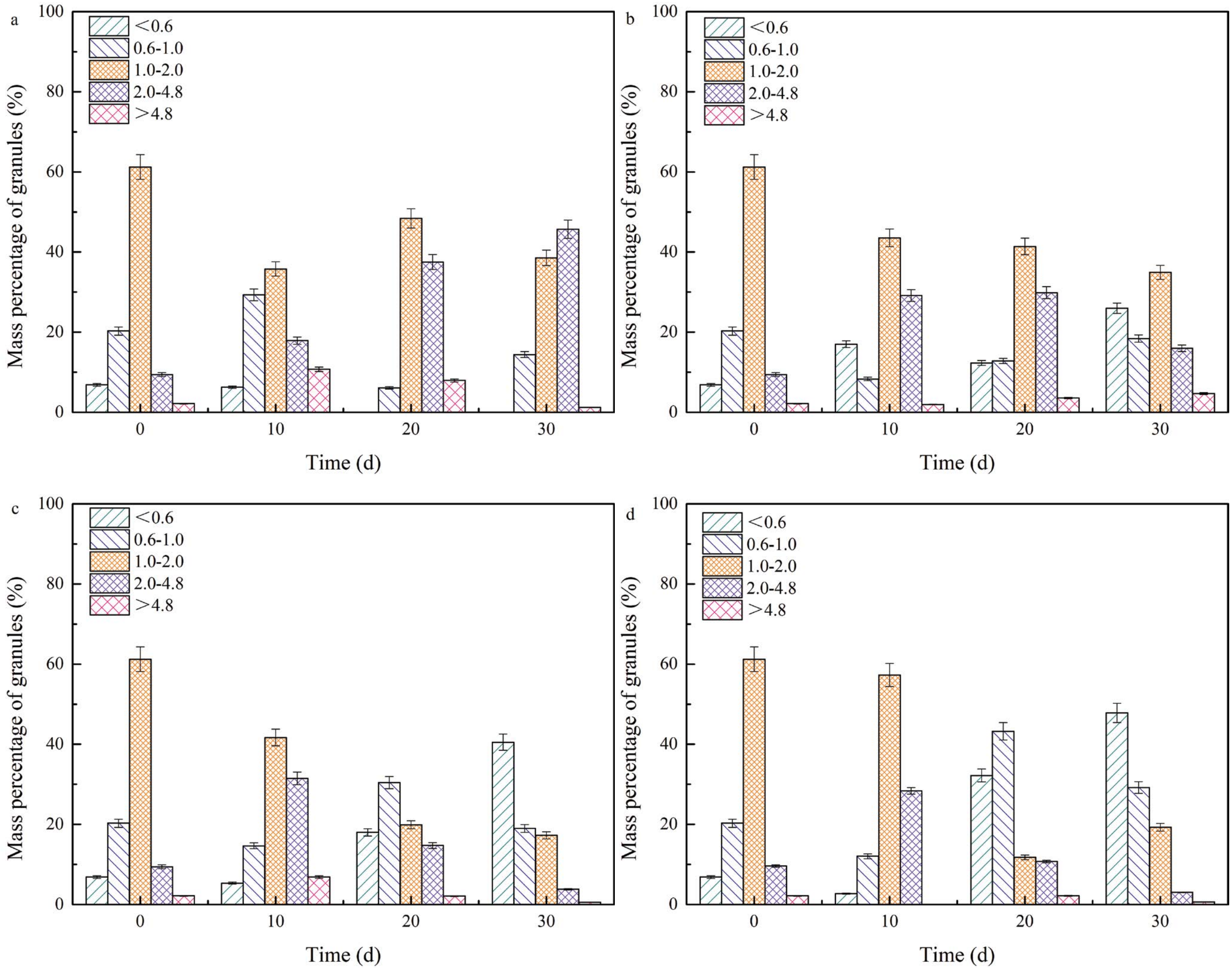

Fig. 4. Change in the mass percentage of granules with different particle sizes during operation: (a) R_N, (b) R_{NN}, (c) R_{NP}, and (d) R_{NNP}.

trend. These results indicate that the mass percentage of granules gradually decreased with increasing NO_2^- and ClO_4^- concentrations. Granules consist of a multitude of bacteria, EPS, and inorganic minerals [30]. DB maintain good performance at low concentrations of coexisting anions, but not at high concentrations of coexistent anions [31,32]. Previously, researchers have found that the denitrifying community changed greatly, sometimes even losing function, after exposure to high salinity [32]. Thus, the mass percentage of granules decreased because of the death of a large amount of bacteria.

3.2.3. Shear sensitivity of DGS

K_{SS} also significantly influences the long-term stability of sludge reactor operation [3,33,34], in which the smaller the K_{SS}, the better the granule stability. The K_{SS} values of the four reactors during operation are shown in Fig. 5. In R_N, the K_{SS} in the three phases were 0.00300 ± 0.00015, 0.00380 ± 0.00019, and 0.00400 ± 0.00020, respectively, indicating that K_{SS} maintained stability in each phase, which suggested that the granules had excellent shear stability.

In R_{NN}, the K_{SS} in the three phases were 0.00198 ± 0.00040, 0.00800 ± 0.00040, and 0.01200 ± 0.00060, respectively. Compared with R_N, the K_{SS} of R_{NN} decreased by approximately 0.00102 in phase I. Then, when the NO_2^- concentration increased to 300 mg L^{-1} in phase II, the K_{SS} slightly increased to approximately 0.00420. Finally, when the NO_2^- concentration increased to 450 mg L^{-1} in phase III, the K_{SS} increased by approximately 0.00800. Thus, the K_{SS} obviously increased when the NO_2^- concentration increased from 150 to 300 mg L^{-1}. Meanwhile, when the NO_2^- concentration increased again to 450 mg L^{-1}, the K_{SS} only slightly increased. These results indicate that the shear stability of the granules gradually weakened with the increasing NO_2^- concentration.

In R_{NP}, the K_{SS} values in the three phases were 0.00480 ± 0.00024, 0.02100 ± 0.00105, and 0.03700 ± 0.00185, respectively. Compared with R_N, the K_{SS} value in R_{NP} increased by only approximately 0.00180 in phase I. When the ClO_4^- concentration increased to 300 mg L^{-1} in phase II, the K_{SS} increased by approximately 0.01720. Finally, when the ClO_4^- concentration increased to 900 mg L^{-1} in phase III, the K_{SS} increased to approximately 0.03300. These results indicate that the shear stability of the granules significantly weakened with increasing ClO_4^- concentration.

In R_{NNP}, the K_{SS} values in the three phases were 0.00450 ± 0.00023, 0.02700 ± 0.00135, and 0.05000 ± 0.00250, respectively. Compared with R_N, the K_{SS} of R_{NNP} increased by approximately 0.00150 when the NO_2^- concentration was 150 mg L^{-1} and the ClO_4^- concentration was 100 mg L^{-1} in phase I. When the NO_2^- and ClO_4^- concentrations were 300 mg L^{-1} in phase II, K_{SS} increased by approximately 0.02320 Finally, when the NO_2^- concentration was 450 mg L^{-1} and the ClO_4^- concentration was 900 mg L^{-1} in phase III, K_{SS} increased by approximately 0.04600. These results indicate that the coexistence of NO_2^- and ClO_4^- adversely affects the shear stability of the granules. In addition, ClO_4^- has a greater impact on the stability of granules than NO_2^-.

3.3. Surface characteristics of DGS

EPS, which are secreted by a multi-species community of microorganisms, mainly consist of PN, PS, and other substances [15]. EPS also protect microorganisms under harsh environmental conditions [35]. The EPS, PN, PS, and PN/PS values of the four reactors during operation are shown in Fig. 6.

EPS accounted for 78.15 ± 3.90 mg g-VSS^{-1}, 83.82 ± 4.19 mg g-VSS^{-1}, and 88.49 ± 4.42 mg g-VSS^{-1} in R_N in the three phases, respectively, showing a gradually increasing trend, which may be related to increases in biomass. Meanwhile, the EPS contents of the other reactors gradually increased with increasing NO_2^- and ClO_4^- concentrations in phases I and II, thereby confirming that bacteria secreted excessive EPS to counteract the increased NO_2^- and ClO_4^- concentrations. Plasmolysis cannot occur when treating saline wastewater, which is related to EPS [36]. With increasing coexisting NO_2^- and ClO_4^- concentrations (phase III), the EPS contents decreased. Thus, one of the main drawbacks of bacteria growth was the difficult living environment, which resulted in cell death.

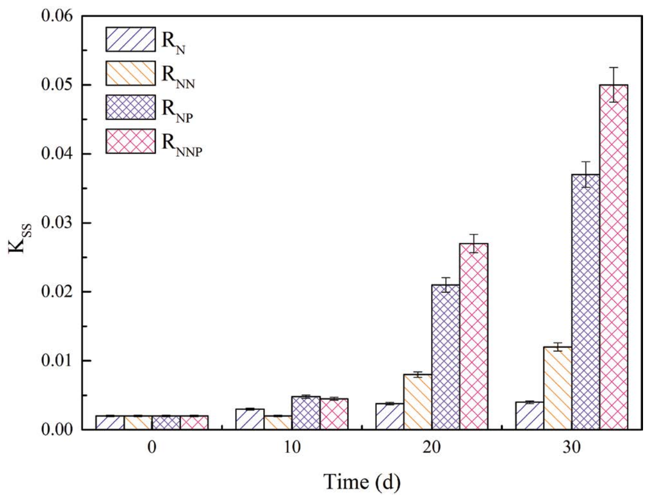

Fig. 5. Change in K_{SS} during operation of R_N, R_{NN}, R_{NP}, R_{NNP}.

In addition, the decrease in EPS concentration weakened the shear strength of the granules, leading to an increasing K_{SS}.

The PN and PS trends are shown in Fig. 6. The PN concentrations of the four reactors during operation first increased and then decreased. A previous study showed that PN was beneficial to the formation and stability of granules as it effectively changed the cell surface's hydrophobicity and settling ability [4]. The trend of PN was similar to that of the EPS. In addition, the PS in the EPS was more abundant than in the PN, which is consistent with previous studies [15]. Thus, when coexisting anions (NO_2^- and ClO_4^-) were present in the reaction system, the bacteria secreted a large amount of PS in response to the adverse environment. The PN/PS of the four reactors during operation gradually decreased with increasing NO_2^- and ClO_4^- concentrations. The stability of the granules decreased when the coexisting NO_2^- and ClO_4^- reached certain concentrations, resulting in a deteriorating granule shear stability.

3.4. Correlation analysis between reactor performance and granular sludge characteristics

The characteristics of the DGS, which are closely related to the performance of the reactor, were affected by the composition and concentration of the influent. To further explore the influence of coexisting NO_2^- and ClO_4^-, the reactor performance and DGS characteristics analyzed using SPSS data analysis software (Table 2). The results showed that the Pearson correlation coefficient between NRR and K_{SS} reached up to –0.991 at a 0.01 level, indicating that they are significantly negatively correlated. Thus, the presence of coexisting NO_2^- and ClO_4^- leads to a change in the K_{SS} value of the granules, which leads to the inhibition of NO_3^- removal [18]. In addition, the Pearson correlation coefficient between SNRR and PN reached –0.959 at a level of 0.05, which indicates that they are significantly positively correlated.

Given these results, the following effects of the coexisting anions on the characteristics of DGS were determined. First, the presence of NO_2^- and ClO_4^- coexisting ions put bacteria in an unfavourable environment, leading to a large amount of EPS secretion. Subsequently, the granule characteristics slightly deteriorated as a result of EPS protection, which caused a decrease in the biomass and particle size distribution and an increase in the K_{SS}. Second, as the concentration of coexisting NO_2^- and ClO_4^- increased, the granule characteristics deteriorated. Thus, the granules disintegrated and flowed out with the effluent, revealing an increase in K_{SS} and a decrease in EPS. Therefore, the reactor effluent deteriorated.

4. Conclusions

As a result of our experiments, the NRR decreased with increasing NO_2^- concentration from 150 to 300 mg L^{-1}. However, the NRR increased at an NO_2^- concentration of 450 mg L^{-1}. Meanwhile, with increasing ClO_4^- concentration (100–900 mg L^{-1}), the NRR gradually decreased. In the presence of NO_2^- and ClO_4^-, the decrease in biomass, disintegration of granules, increase in K_{SS}, and decrease in EPS concentration deteriorated the granules characteristics, eventually leading to a decrease in the NRR. Further, the

Table 2
Pearson correlation coefficient between reactor performance and granular sludge characteristics in the four reactors in the three phases

	NRR	SNRR	RSD	K_{SS}	EPS	PN	PS	PN/PS	MLVSS	SVI
NRR										
SNRR	0.742									
RSD	–0.355	–0.586								
K_{SS}	–0.991[b]	–0.826	0.429							
EPS	0.353	0.858	–0.786	–0.475						
PN	0.539	0.959[a]	–0.683	–0.649	0.966[a]					
PS	0.742	0.345	–0.592	–0.703	0.161	0.210				
PN/PS	0.316	0.829	–0.271	–0.428	0.805	0.874	–0.238			
MLVSS	0.779	0.237	–0.323	–0.708	–0.073	0.035	0.952[a]	–0.329		
SVI	0.934	0.578	–0.5	–0.907	0.268	0.395	0.933	0.037	0.93	

[a]Significantly correlated at 0.05 levels (both sides);
[b]Significantly correlated at 0.01 levels (both sides).

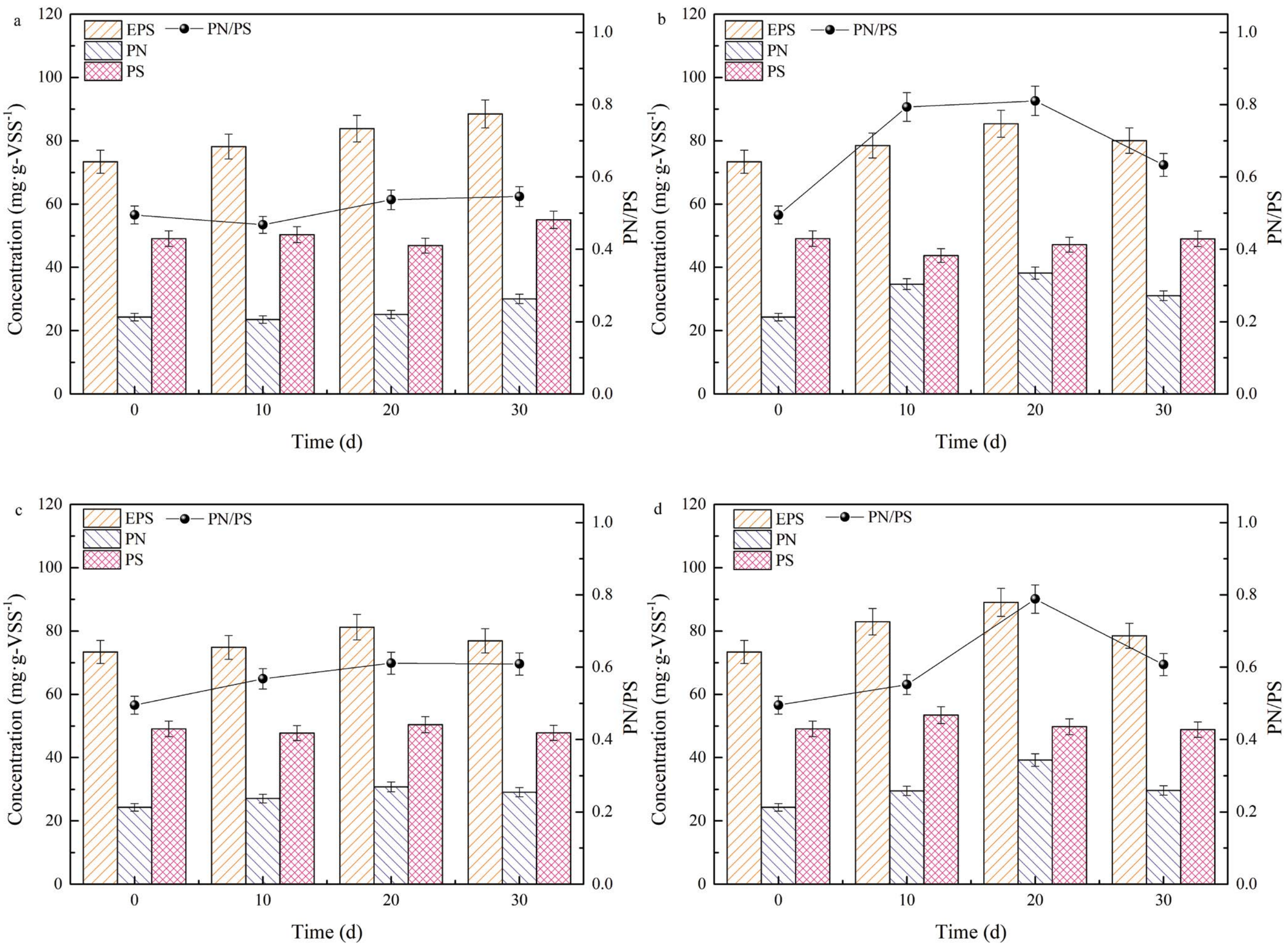

Fig. 6. Change in the EPS, PN, PS and PN/PS during operation: (a) R_N, (b) R_{NN}, (c) R_{NP}, and (d) R_{NNP}.

correlation analysis showed that NRR and K_{SS} were significantly negatively correlated. This study provides a new understanding of nitrate removal by DGS in the coexistent anions.

Acknowledgements

This work was supported by the National Natural Science Foundation of China (Grant No. 51678387); the

Talented Training Project of Hebei Province (Grant No. A201902019); Key Project of Hebei Province Higher Education Science and Technology Research Foundation (ZD2019038); Youths Project of Hebei Province Higher Education Science and Technology Research Foundation (QN2018062); Key project of Tianjin Education Commission Scientific Research Plan (Grant No. 2017KJ056) and Key project of Tianjin Natural Science Foundation (Grant No. 17JCZDJC39300).

References

[1] Z. Wang, Y.H. Jiang, M.K. Awasthi, J. Wang, X.G. Yang, A. Amjad, Q. Wang, A.H. Lahori, Z.Q. Zhang, Nitrate removal by combined heterotrophic and autotrophic denitrification processes: impact of coexistent ions, Bioresour. Technol., 250 (2018) 838–845.

[2] E. Sahinkaya, A. Yurtsever, A. Özgür, D. Ucar, Z.W. Wang, Sulfur-based autotrophic denitrification of drinking water using a membrane bioreactor, Chem. Eng. J., 268 (2015) 180–186.

[3] Y.Q. Xue, J.B. Guo, J. Lian, Y.Y. Zhang, C. Zhang, Y. Zhao, Effect of a higher hydraulic shear force on denitrification granulation in upflow anoxic sludge blanket reactors, Biochem. Eng. J., 105 (2016) 136–143.

[4] W.Y. Niu, J.B. Guo, J. Lian, H.H. Ngo, H.Y. Li, Y.Y. Song, H.B. Li, P.N. Yin, Effect of fluctuating hydraulic retention time (HRT) on denitrification in the UASB reactors, Biochem. Eng. J., 132 (2018) 29–37.

[5] J.P.S. Sukias, J.B.K. Park, R. Stott, C.C. Tanner, Quantifying treatment system resilience to shock loadings in constructed wetlands and denitrification bioreactors, Water Res., 139 (2018) 450–461.

[6] X. Zhou, Y.P. Han, X.S. Guo, Identification and evaluation of SND in a full-scale multi-channel oxidation ditch system under different aeration modes, Chem. Eng. J., 259 (2015) 715–723.

[7] D.C. Catling, M.W. Claire, K.J. Zahnle, R.C. Quinn, B.C. Clark, M.H. Hecht, S. Kounaves, Atmospheric origins of perchlorate on Mars and in the Atacama, J. Geophys. Res. 115 (2010) 1–15.

[8] W. Song, B.Y. Gao, X. Xu, F. Wang, N. Xue, S.L. Sun, W.C. Song, R.B. Jia, Adsorption of nitrate from aqueous solution by magnetic amine-crosslinked biopolymer based corn stalk and its chemical regeneration property, J. Hazard. Mater., 304 (2016) 280–290.

[9] X.S. Cao, D. Qian, X.Z. Meng, Effect of pH on nitrite accumulation during wastewater denitrification, Environ. Technol., 34 (2013) 45–51.

[10] C. Glass, J. Silverstein, J. Oh, Inhibition of denitrification in activated sludge by nitrite, Water Environ. Res., 69 (1997) 1086–1093.

[11] D.J. Wan, Y.D. Liu, Y.Y. Wang, H.J. Wang, S.H. Xiao, Simultaneous bio-autotrophic reduction of perchlorate and nitrate in a sulfur packed bed reactor: kinetics and bacterial community structure, Water Res., 108 (2017) 280–292.

[12] W. Song, B.Y. Gao, H.L. Wang, X. Xu, M. Xue, M.C. Zha, B. Gong, The rapid adsorption-microbial reduction of perchlorate from aqueous solution by novel amine-crosslinked magnetic biopolymer resin, Bioresour. Technol., 240 (2017) 68–76.

[13] S.W. Van Ginkel, R. Lamendella, W.P. Kovacik, J.W. Santo Domingo, B.E. Rittmann, Microbial community structure during nitrate and perchlorate reduction in ion-exchange brine using the hydrogen-based membrane biofilm reactor (MBfR), Bioresour. Technol., 101 (2010) 3747–3750.

[14] Z.G. Chen, X.J. Wang, Y.Y. Yang, M.W. Mirino, Y.L. Yuan, Partial nitrification and denitrification of mature landfill leachate using a pilot-scale continuous activated sludge process at low dissolved oxygen, Bioresour. Technol., 218 (2016) 580–588.

[15] C.J. Tang, P. Zheng, C.H. Wang, Q. Mahmood, J.Q. Zhang, X.G. Chen, L. Zhang, J.W. Chen, Performance of high-loaded ANAMMOX UASB reactors containing granular sludge, Water Res., 45 (2011) 135–144.

[16] G.P. Sheng, H.Q. Yu, X.Y. Li, Stability of sludge flocs under shear conditions, Biochem. Eng. J., 38 (2008) 302–308.

[17] M. Verawaty, S. Tait, M. Pijuan, Z.G. Yuan, P.L. Bond, Breakage and growth towards a stable aerobic granule size during the treatment of wastewater, Water Res., 47 (2013) 5338–5349.

[18] L.H. Mikkelsen, K. Keiding, The shear sensitivity of activated sludge: an evaluation of the possibility for a standardised floc strength test, Water Res., 36 (2002) 2931–2940.

[19] APHA, Standard Methods for the Examination of Water and Wastewater, 20th ed., American Public Health Association, Washington, DC, USA, 1998.

[20] S.S. Adav, D.J. Lee, Extraction of extracellular polymeric substances from aerobic granule with compact interior structure, J. Hazard. Mater., 154 (2008) 1120–1126.

[21] M.M. Bradford, A rapid and sensitive method for the quantitation of microgram quantities of protein utilizing the principle of protein-dye binding, Anal. Biochem., 72 (1976) 248–254.

[22] L. Xia, X.M. Li, W.H. Fan, J.L. Wang, Heterotrophic nitrification and aerobic denitrification by a novel *Acinetobacter* sp. ND7 isolated from municipal activated sludge, Bioresour. Technol., 301 (2020) 122749, doi: 10.1016/j.biortech.2020.122749.

[23] J. Oh, J. Silverstein, Acetate limitation and nitrite accumulation during denitrification, J. Environ. Eng., 125 (1999) 234–242.

[24] K. Calder, K.A. Burke, J. Lascelles, Induction of nitrate reductase and membrane cytochromes in wild type and chlorate resistant *Paracouccis denitrificans*, Arch. Microbiol., 126 (1980) 149–153.

[25] H. Körner, W.G. Zumft, Expression of denitrification enzymes in response to the dissolved oxygen level and respiratory substrate in continuous culture of *Pseudomonas stutzeri*, Appl. Environ. Microbiol., 55 (1989) 1670–1676.

[26] S. Chen, C. Juaw, S. Cheng, Nitrification and denitrification of high-strength ammonium and nitrite wastewater with biofilm reactors, Water Sci. Technol., 23 (1991) 14–17.

[27] S. Sevda, T.R. Sreekishnan, N. Pous, S. Puig, D. Pant, Bioelectroremediation of perchlorate and nitrate contaminated water: a review, Bioresour. Technol., 255 (2018) 331–339.

[28] A. Ghosh, K. Pakshirajan, P.K. Ghosh, N.K. Sahoo, Perchlorate degradation using an indigenous microbial consortium predominantly *Burkholderia* sp., J. Hazard. Mater., 187 (2011) 133–139.

[29] P.N. Yin, J.B. Guo, S.M. Xiao, Z. Chen, Y.Y. Song, X.N. Ren, Rapid of cultivation dissimilatory perchlorate reducing granular sludge and characterization of the granulation process, Bioresour. Technol., 276 (2019) 260–268.

[30] J.E. Schmidt, B.K. Ahring, Granular sludge formation in upflow anaerobic sludge blanket (UASB) reactors, Biotechnol. Bioeng., 49 (1996) 229–246.

[31] Y. Miao, R. Liao, X.X. Zhang, B. Liu, Y. Li, B. Wu, A. Li, Metagenomic insights into salinity effect on diversity and abundance of denitrifying bacteria and genes in an expanded granular sludge bed reactor treating high-nitrate wastewater, Chem. Eng. J., 277 (2015) 116–123.

[32] S. Yoshie, H. Makino, H. Hirosawa, K. Shirotani, S. Tsuneda, A. Hirata, Molecular analysis of halophilic bacterial community for high-rate denitrification of saline industrial wastewater, Appl. Microbiol. Biotechnol., 72 (2006) 182–189.

[33] X.M. Chen, Y.W. Liu, L. Peng, B.J. Ni, Perchlorate, nitrate, and sulfate reduction in hydrogen-based membrane biofilm reactor: model-based evaluation, Chem. Eng. J., 316 (2017) 82–90.

[34] T.R. Devlin, A.D. Biase, M. Kowalski, J.A. Oleszkiewicz, Granulation of activated sludge under low hydrodynamic shear and different wastewater characteristics, Bioresour. Technol., 224 (2017) 229–235.

[35] B. Long, C.Z. Yang, W.H. Pu, J.K. Yang, F.B. Liu, L. Zhang, J. Zhang, K. Cheng, Tolerance to organic loading rate by aerobic granular sludge in a cyclic aerobic granular reactor, Bioresour. Technol., 182 (2015) 314–322.

[36] S.F. Corsino, M. Capodici, F.D. Pippo, V. Tandoi, M. Torregrossa, Comparison between kinetics of autochthonous marine bacteria in activated sludge and granular sludge systems at different salinity and SRTs, Water Res., 148 (2019) 425–437.

Supporting information

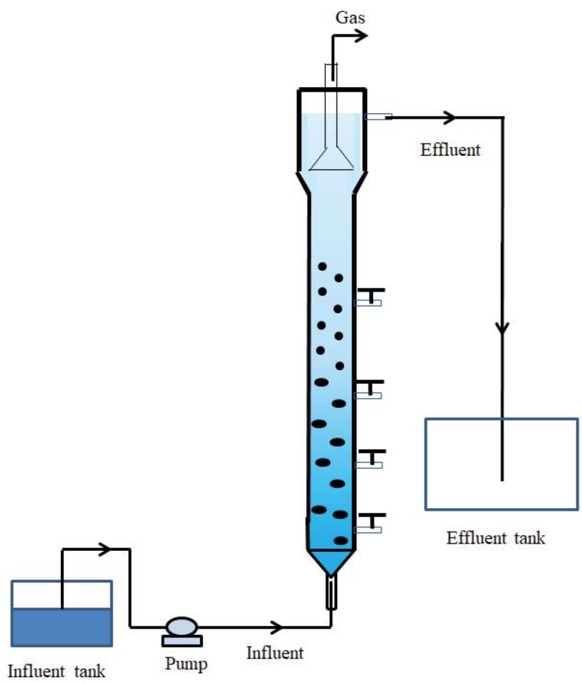

Fig. S1. Graphical scheme of UASB reactor.

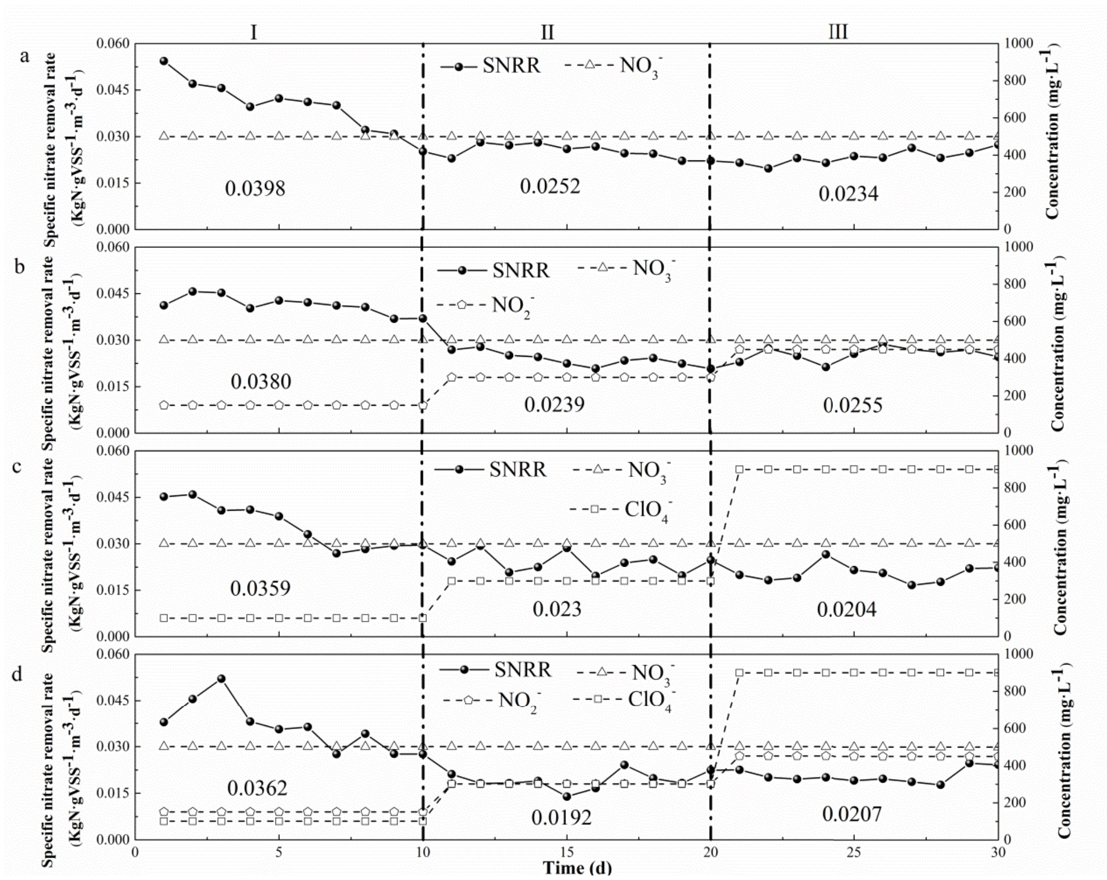

Fig. S2. Change in the SNRR during operation: (a) R_N, (b) R_{NN}, (c) R_{NP}, and (d) R_{NNP}.